COMMUNICATION

Controlled Synthesis of Large-Scale, Uniform, Vertically Standing Graphene for High-Performance Field Emitters

Lili Jiang, Tianzhong Yang, Fei Liu, Jing Dong, Zhaohui Yao, Chengmin Shen, Shaozhi Deng, Ningsheng Xu, Yunqi Liu,* and Hong-Jun Gao*

Graphene, a two-dimensional (2D) sheet consisting of sp²-hybridized carbon atoms, has attracted enormous attention during recent years because of its outstanding materials characteristics[1–3] and promising technological applications.[4–12] While devices with graphene sheets lying flat on substrates have been investigated extensively, the alternative configuration invovling vertically standing graphene (VSG) films on substrates has been lacking but possesses many unique potential applications, such as supercapacitors and biosensors.[13,14] Because plenty of exposed edge planes exist in such VSG devices, which can also potentially provide a high density of individual field emission sites, application of VSG films towards high-efficiency field emitters has already been suggested.[15–17] However, a few major challenges need to be addressed in order to achieve excellent VSG-based field emitters possessing a low turn-on field, low threshold field, high enhancement factor, and good stability, including the reliable fabrication of large-scale uniform VSG films with high yield and precise engineering of interfacial contact with substrates.

Here, we report an approach to develop wafer-sized and uniform VSG films on copper (Cu) foil by using a microwave-plasma chemical vapor deposition (MP-CVD) system with high reproducibility. While Cu has been applied as substrate for large-area graphene and uniform growth by methods such as thermal CVD, the growth mechnism of VSG on Cu remains ambiguous.[13–15] It has been demonstarted that as-prepared VSG films containing large-sized graphene sheets with atomically thin edges can significantly contribute to the emission current for field-emission displays.[18] In addition, the copper substrate represents a convenient and economic collector electrode for field emitters. In this work, the growth mechanism of VSG films on Cu substrates is also elucidated. We further demonstrate that the morphology of VSG films can be controlled by optimizing the growth conditions, such as growth time, CH_4 flow rate, and ratio of CH_4/H_2. Lastly, field-emission devices based on Cu-VSG films are shown to possess a low turn-on electric field of 1.3 V μm^{-1}, a low threshold field of 3.0 V μm^{-1} and a large field-enhancement factor of 1.1×10^4, confirming the high quality of the VSG films, as well as their promising application for large-area field emitters.

Figure 1a,b show the typical surface topography of a VSG film after 2 min of growth under 6.0 Torr with a mixture of CH_4 and H_2 (10 sccm:50 sccm). A large quantity of carbon edges can be found as compared with planar graphene. The cross-sectional scanning electron microscopy (SEM) image of VSG on the Cu substrate (Figure 1c) demonstrates that the as-grown graphene sheets are nearly perpendicular to the substrate. The height of each vertical sheet is about 1.6 μm. Figure 1d,e show transmission electron microscopy (TEM) images of VSG, suggesting that the graphene sheets have smooth and thin edges. The selected-area electron diffraction (SAED) pattern (inset of Figure 1d) further confirms the high crystal quality by the hexagonal diffraction patterns. High-resolution transmission electron microscopy (HR-TEM) images, as shown in Figure 1f and Figure 1g, reveal that the edges are terminated with single-layer graphene and four-layer graphene, respectively. The interlayer spacing between two neighboring monolayer sheets is about 0.364 nm, which is larger than that of graphite, and is most likely caused by reduced interactions between them. More evidence can be found from Raman characterization. The layers counted on the edges from the TEM images imply that the VSG films terminate with a thickness corresponding to few-layer graphene or less.

From the optical image (**Figure 2**a) and SEM images under different magnifications (Figure 2b,c), it is clear that this VSG film uniformly grew over the whole substrate with a diameter up to 15 mm, which was not facile on Si or SiO_2 in our system (Supporting Information, Figure S1). The "wafer-scaled" VSG films would be important for further applications of, for example, pattern-arrayed devices (Supporting Information, Figure S1). Growth on larger wafers is currently limited by the

L. L. Jiang, Dr. T. Z. Yang, Dr. C. M. Shen, Prof. H. J. Gao
Beijing National Laboratory of
Condensed Matter Physics
Institute of Physics
Chinese Academy of Sciences
Beijing 100190, P. R. China
E-mail: hjgao@iphy.ac.cn
Dr. F. Liu, Prof. S. Z. Deng, Prof. N. S. Xu
State Key Laboratory of Optoelectronic Materials and Technologies
Guangdong Province Key Laboratory of Display
Material and Technology
and School of Physics and Engineering
Sun Yat-sen University
Guangzhou 510275, P. R. China
J. Dong, Prof. Z. H. Yao
School of Aerospace
Tsinghua University
Beijing 100084, P. R. China
Prof. Y. Q. Liu
Beijing National Laboratory for Molecular Sciences
Key Laboratory of Organic Solids
Institute of Chemistry
Chinese Academy of Sciences
Beijing 100190, P. R. China
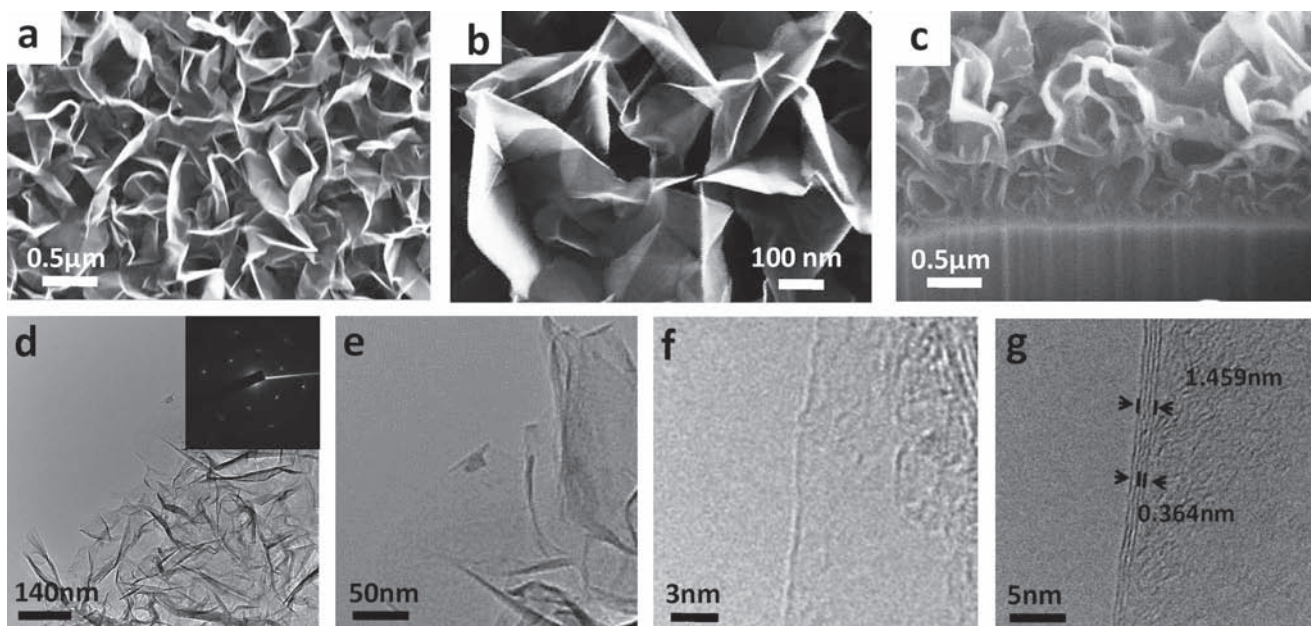E-mail: liuyq@iccas.ac.cn

Figure 1. a) SEM image of VSG grown on copper foil under growth conditions of: a H_2/CH_4 ratio of 50 sccm/10 sccm, a pressure of 6.0 Torr, and a growth time of 2 min. The scale bar is 500 nm. b) Magnified SEM image of the VSG film. c) Cross-sectional SEM image of VSG on a Cu substrate. d,e) TEM images of VSG (with SAED of hexagonal patterns in the inset of (d), showing that the nanosheet has a sharp edge with an open graphitic edge plane. f,g) HR-TEM images of VSG with single-layer graphene and four-layer graphene edges, respectively.

size of the sample holder in our home-made CVD chamber. Raman maps in several randomly selected areas also confirm the uniformity of VSG films (Supporting Information, Figure S2). Furthermore, growth on Cu substrates showed a much higher growth rate than on Ni,[13] Si,[14] and other metal or non-metal substrates. Graphene sheets with an average size of 1.5 μm could be obtained after just 2 min under the above experimental conditions, while several tens of minutes would be needed for a
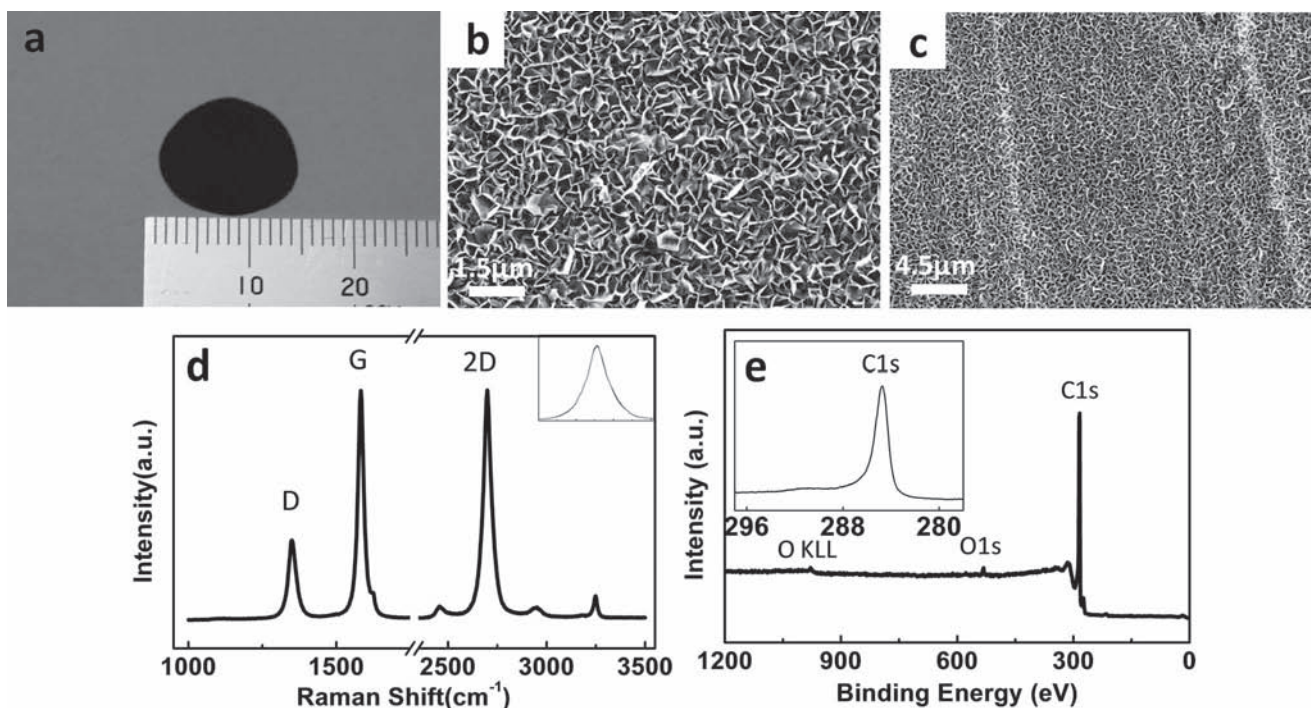

Figure 2. a) Optical image of VSG film on a copper substrate with a diameter of ≈15 mm. b,c) SEM images of VSG film with different magnifications. d) Raman spectrum of VSG. The inset shows a single Lorentz shape fitting of the 2D band. e) XPS of the VSG sample, with the C1s spectrum in the inset.

smaller size on other substrates, according to previous reports and our controlled experiments.

To identify the composition, crystal structure, and valence states, further characterizations of VSG films by means of Raman spectroscopy (Figure 2d), X-ray photoelectron spectroscopy (XPS) (Figure 2e) and electron energy-loss spectroscopy (Supporting Information, Figure S3) were carried out. Raman spectroscopy can provide information on the number of layers, the defect density, and the layer stacking in our VSG samples. Figure 2d shows a typical Raman spectrum of as-grown VSG with four major bands: G bands appear at the expected position, ≈1582 cm^{-1}, with a full width at half-maximum (FWHM) of 23 cm^{-1}, which corresponds to the doubly degenerate phonon mode (E_{2g}) at the Brillouin zone center. The 2D band is at ≈2700 cm^{-1} and has a broadened FWHM of 49 cm^{-1}, which is associated with second-order zone-boundary phonons. This finding indicates that the few-layer graphene does not exhibit Bernal AB stacking of graphene layers, and that the layers are randomly rotated with respect to one another along the *c* axis.[19] The reduction of the interlayer interaction between the graphene layers results in similar features in the Raman spectra as seen for monolayer graphene, which may offer advantageous electrical properties for device applications. The broadened line width of the 2D band can be attributed to the relaxation of double resonance Raman selection rules related to the random orientation of the graphene layers. The ratio of the G band to 2D band intensity is nearly 1, suggesting that as-synthesized materials should be few-layer graphene. The high-intensity D band of this VSG film at ≈1350 cm^{-1} is possibly due to the large fraction of edge carbons serving as defects by breaking the translational symmetry of the lattice. As a result, all of the evidence from the Raman spectra reveal that our samples consisted of randomly stacked few-layer graphene sheets with a large portion of edges on the top.

The X-ray photoelectron spectroscopy (XPS) technique was used to investigate the chemical composition and valence states of the VSG films. Figure 2e is a representative XPS spectrum of VSG, showing a strong C 1s peak at 284.8 eV, a small O 1s peak at 532.7 eV, and a weak O KLL Auger band between 970–980 eV. Except for some oxygen adsorbates on the surface, no other elements were found in the film. The concentrations of C and O elements in the film were about 98.3% and 1.7%, respectively. The formation of such oxygen adsorbates is believed to result from physical and/or chemical adsorption of oxygen, mainly on the edge defects at room temperature, when the sample was exposed to ambient conditions. In a high-resolution asymmetric C 1s spectrum (inset of Figure 2e), the tail between 286 eV and 290 eV is due to C–O, C=O, and energy-loss "shake-up" features.[20,21]

Several similar materials on substrates of such as Ni, Si, and SiO$_2$ have been achieved.[13–15] However, the growth mechanism of VSG film on Cu substrate has not been clear. To elucidate the growth mechanism of VSG films on Cu substrates, the evolution of VSG film was monitored by varying the growth time under otherwise the same conditions. We prepared samples with growth periods varying from 30 s to 2 min under 6.0 Torr of CH$_4$/H$_2$ with a fixed ratio (5:50 sccm). We found that when the growth time was increased to 1 min, a planar film containing wrinkles or ripples was obtained (**Figure 3**a). The

Raman spectra of such a planar film (see Supporting Information, Figure S4a) demonstrate that this film should be turbostratic graphite since the 2D peak could be fitted with a single Lorentzian lineshape with a broadened FWHM of 61 cm^{-1}.[19] However, the high intensity of the D peak suggests a poor quality of the multilayer graphene film. From the zoomed-in SEM image (Figure 3b), plenty of carbon grains can be observed, which possibly contributed to the high peak intensity of the D band in the Raman spectra. As the growth time was increased to 2 min, the VSG was fully developed (Figure 3c). This observation suggests that flat epitaxial layer was formed first, and then a transition to a 3D island growth mode could take place after a certain critical thickness, following the Stranski–Krastanov growth model.[22]

Based on the above experimental findings, we developed a model (Figure 3d–h) to understand the growth of VSG films on copper surfaces in the MP-CVD system: In the initial stage of VSG growth, the feeding gas (CH$_4$) was decomposed to carbon atoms or benzene rings with saturated or unsaturated carbon–hydrogen bonds by the microwaves, serving as building blocks (Figure 3d). Once the supersaturation condition was reached, the precursors could adsorb on the Cu substrates and begin to nucleate. By using copper-foil substrates as a surface-active agent to reduce the surface free energy, an increased island density was achieved, and thus two-dimensional growth was enhanced.[23,24] Firstly, a few monolayers with random stacking were formed (Figure 3e), followed by the growth of carbon clusters, as revealed in Figure 3b. Subsequent layer-growth mode was unfavorable due to the following two reasons: 1) because of sufficient accumulation of strain energy in the system, the intermediate layer may not be able to continue to form bulk crystal, and thus cause a transition from 2D complete films to 3D clusters beyond a critical layer thickness;[24] indeed, we found a remarkable blueshift of the 2D peak (2713 cm^{-1}) compared with exfoliated graphene on SiO$_2$ (2683 cm^{-1}) (Supporting Information, Figure S4b), which agreed well with the existence of compressive strain in planar few-layer graphene (Supporting Information, Figure S4a).[25] 2) In this ion-assisted deposition process, the precursors possessing high energy may create defects on the film surface that could become new nucleation sites due to a higher binding energy for growth. Both the extreme strain and the defects of the as-deposited film (Figure 3f) finally led to a vertical growth in the 3D clusters (Figure 3g). In addition, an enhancement in carbon-atom mobility from the microwave energy could ensure growth along the vertical-graphene sheet because these atoms would reach the edges more frequently and thus diffuse outwards. As the size of the graphene sheets increases, they interact with neighboring sheets via van der Waals forces, leading to overall rigidity for oriented growth (Figure 3h). This rigidity further assures that the graphene sheets can keep growing along the original vertical direction.

The performance of VSG film usually is dependent on its morphology, such as the surface area and the thickness of edges. Thus, in order to obtain VSG films with a large size and thin-edge graphene sheets, we modulated the morphology by varying the growth time, CH$_4$ flow rate, and the ratio of CH$_4$ to H$_2$, based on our proposed growth mechanism. **Figure 4**a–f show SEM images of the VSG films with increasing CH$_4$ flow

Materials
Views
www.MaterialsViews.com

ADVANCED
MATERIALS
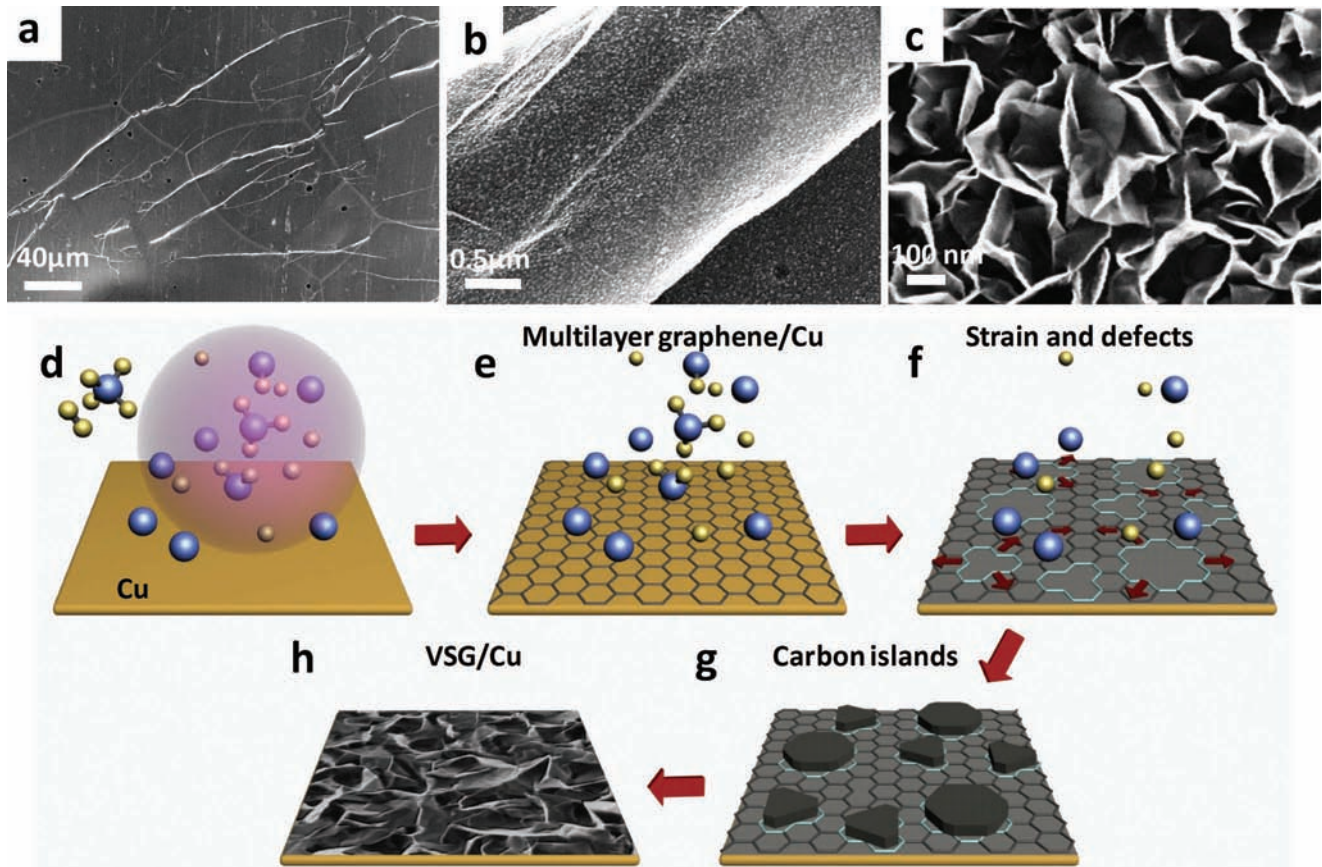www.advmat.de

COMMUNICATION

Figure 3. a) SEM image of the former state of VSG grown on copper foil under growth conditions of: H_2/CH_4 ratio of 50 sccm/5 sccm, pressure of 6.0 Torr, and growth time of 1 min. b) Magnified SEM image of (a). c) SEM image of VSG with growth time increasing to 2 min. d–h) Schematic growth process of VSG film on copper substrate in an MP-CVD system. d) Breakage of carbon–hydrogen bonds by microwaves. e) Formation of multilayer graphene on a Cu surface. f) Strain and defects on 2D graphene film after a period of growth. g) Transition from 2D to 3D growth due to accumulated strain and defects. h) Development of a VSG film on a Cu substrate due to high mobility of the carbon atoms and van der Waals force between neighboring graphene sheets.
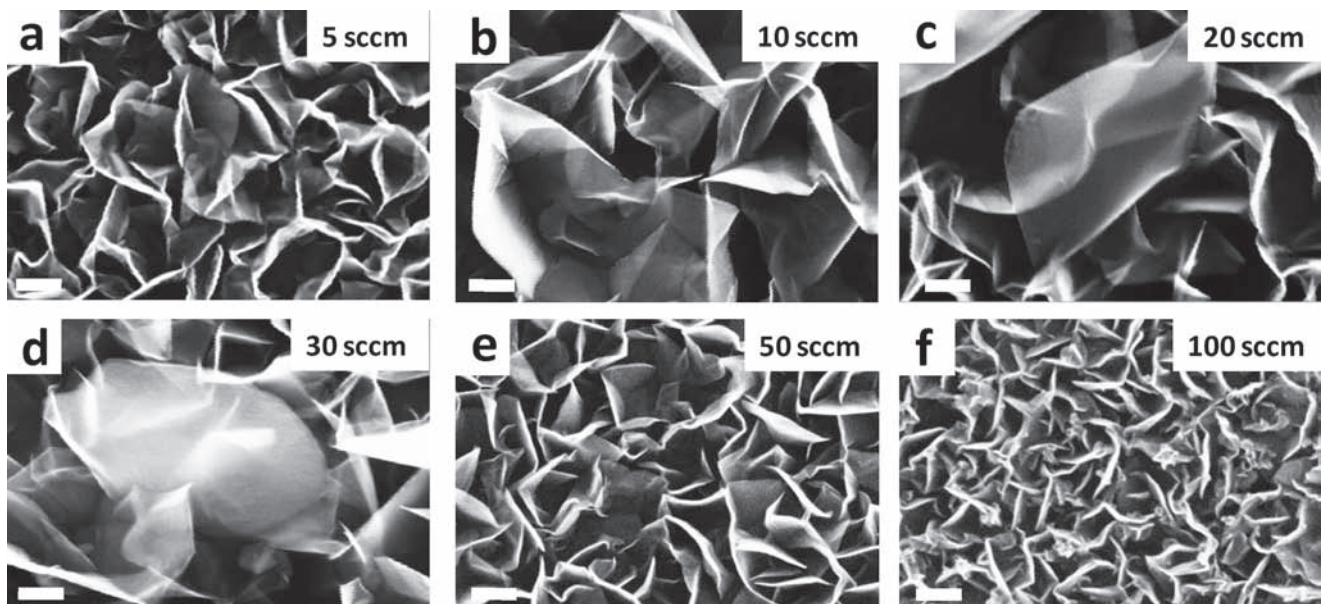

Figure 4. a–f) SEM images of VSG growth with an increase of CH_4 flux from 5 sccm to 100 sccm while maintaining a constant H_2 flux of 50 sccm. The growth pressure is 6.0 Torr. The scale bars in all six images are 100 nm.
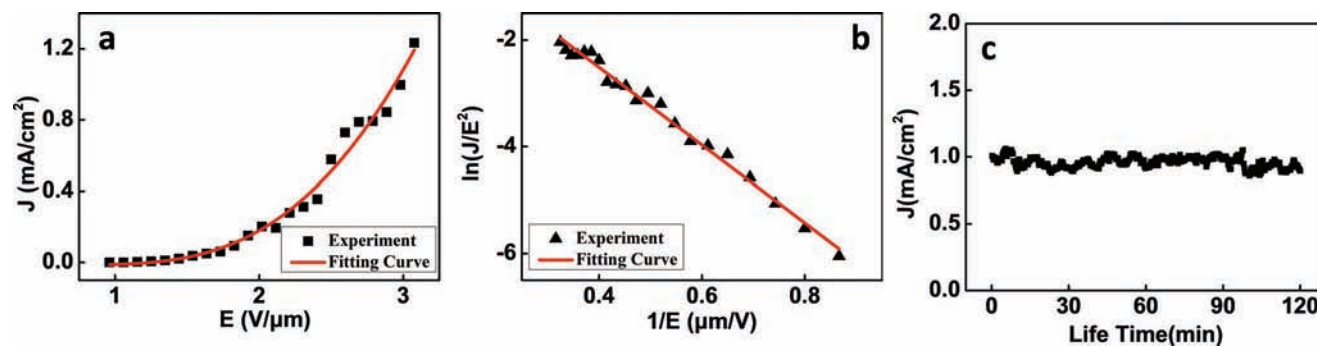
COMMUNICATION

Figure 5. a) Typical plots of electron-emission current density (J) as a function of applied electric field (E) for the VSG film. b) Corresponding F–N plots. c) Stability of emission current of the VSG film grown on copper substrate.

rates from 5 sccm to 100 sccm, while keeping the H_2 flux constant. The size of the graphene sheet increased with the increase of the methane flow rate with a maximum at 10 sccm, remained steady between 10 and 30 sccm, and then decreased when increasing CH_4 flow rate further. The corresponding Raman spectra of the samples with different methane flow rates are plotted in Figure S5 in the Supporting Information. We also found that larger CH_4 flow rates usually led to shorter times for nucleation and growth (Supporting Information, Figure S6). According to classical nucleation theory, thin films are often grown away from thermodynamic equilibrium and their morphology becomes determined by the kinetics.[24] A faster generation of carbon monomers, resultant from a larger methane flow rate, could lead to a higher nucleus density and a faster nucleation. An insufficient gas-flow rate could go against the nucleation and growth of samples due to a shortage of the carbon source, while the excessively high density of the crystal nucleus tended to hinder the nucleus from growing into large sizes of graphene sheets, since the interspace between two neighboring nuclei was smaller than that in low-density-nucleation samples. Furthermore, as the methane flow rate increases, the ratio of CH_4 to H_2 is increased, which would reduce the etching effect of the hydrogen plasma and lead to thicker graphene sheets (Figure 4f). However, the overlarge H_2 ratio also led to a small size of the graphene sheets due to the excessive etching effect (Figure 4a). Controlling the dynamic competition between growth and etching turns out ot be the key to obtaining VSG films containing a large size of graphene sheets with atomic thin edges successfully. Under a certain methane flow rate and ratio of CH_4 to H_2, the size of the graphene sheets increases with growth time but exhibits saturation thereafter. An excessive growth time would cause damage to the films (Supporting Information, Figure S7). Thus, we conclude that an appropriate growth time, methane flow rate, and ratio of CH_4/H_2 are crucial for achieving samples with the desired morphology.

To characterize further the quality of our VSG film and explore its possible applications, the field-emission behavior was investigated using a home-made field-emission measurement and analysis system. The anode was an indium tin oxide (ITO)-coated glass, and the Cu foil substrate with VSG was used as the cathode. The interelectrode distance was kept at 520 μm, and the area of the sample was 8 mm × 8 mm. **Figure 5**a

displays the current density (J) as a function of electric field (E) for the as-prepared VSG film (10 sccm CH_4, 2 min growth time). The fabricated field emitter exhibited a low turn-on electric field ($J = 10$ μA cm^{-2}) around 1.3 V μm^{-1} and a low threshold field ($J = 1$ mA cm^{-2}) around 3.0 V μm^{-1}, which were much lower than the values observed in VSG films on a Si substrate or graphene films prepared by the coating method or electrophoretic deposition.[15,26] In addition, a high field-emission current density of 1.3 mA cm^{-2} was also observed with no saturation tendency during the measurement. Fowler–Nordheim (F–N) theory is the most-commonly used model for understanding the electron-emission behavior of various nanostructures,[27,28] in which a good linearity of the F–N plots typically suggests that the cathode material agrees with this model. To investigate the underlying electron-emission mechanism of the VSG film, we further plotted $\ln(J/E^2)$ versus $1/E$, which could be fitted with a linear line shape (Figure 5b) and showed to be in good agreement with the F–N equation. By taking the work function of graphite (≈5 eV), the field-enhancement factor (β) of the VSG film was calculated to be about 1.1×10^4 from the fitting curve, which is among the highest of all graphene-based materials.[17,18,26,29,30] The large enhancement factor allows for sufficient tunneling of electrons from VSG films through barriers, giving rise to a low turn-on voltage. To evaluate the stability of the field-emission current of the VSG films, we recorded the current density of 1 mA cm^{-2} over 120 min. As shown in Figure 5c, no obvious degradation of emission performance was observed.

The excellent field-emission characteristics of VSG films on a copper substrate may be attributed to following factors: firstly, VSG film has plenty of atomic-thick graphene edges. Together with other unique features, such as the high aspect ratio, excellent electrical conductivity, and good mechanical properties of few-layer graphene, it meets all the requirements for an excellent field emitter; secondly, VSG growth on Cu substrates ensures uniform morphology and a high graphene density. Sufficient effective field-emission sites for reducing the turn-on field and increasing the emission current can also be achived; thirdly, the unique growth mode of VSG film on copper substrates may improve the interfacial contact, reduce the resistance between the films and substrates, compared with VSG films on Si substrates or graphene flims prepared by the spray method, and thus improve the field-emission performance; finally, the good

stability of the VSG films may be due to their homogenous surface morphology[26] and good interfacial contact. All of the above factors result in the low turn-on field, low threshold field, high enhancement factor, and excellent current stability, making VSG film a good candidate for a field-emission source.

In summary, we have developed a microwave-plasma CVD process for synthesizing large-scale and uniform VSG films with high quality, high yield, and high growth rate on wafer-scale copper substrates. The growth mechanism of the VSG film on Cu substrate is also discussed in detail for the first time. By optimizing the growth conditions, VSG films with a high surface area and sharp edges can be achieved. These films also exhibit excellent field-emission properties with a low turn-on electric field of 1.3 V μm^{-1}, a low threshold field of 3 V μm^{-1}, a large field-enhancement factor of 1.1×10^4, and good emission stability, suggesting promising applications in energy storage and as field emitters. More efforts on seeking potential applications of such VSG films are in process.

Experimental Section

Synthesis of the VSG was carried out in a home-made, microwave-plasma deposition system. Inductively coupled plasma was generated at the entrance of a 1.2 inch quartz-tube furnace. The typical experimental procedure is summarized as follows: after the sample (quartz) supporter with copper foil was placed, the reaction chamber (quartz tube) was pumped down and then refluxed by H_2 for a certain time to eliminate contamination thoroughly. After the pressure in the chamber reached the expected value and was stable under a certain ratio of CH_4/H_2, the microwave was started and maintained for a a certain period; then, the source of microwave and gas was shut down while the pump continued running for about twenty minutes to ensure that the samples were cooled down to room temperature naturally under vacuum conditions.

SEM images were recorded using a Raith 150 instrument with a working voltage at 10 kV. Raman spectroscopy was performed using a Horiba Jobin Yvon LabRAM HR-800 Raman microscope (λ = 532 nm, power = 1 mW, beam spot = 1 μm) at room temperature and under ambient conditions. HR-TEM analysis and EELS spectra were recorded on a JEOL 2010 instrument operating at 200 kV: samples were scraped off the copper foil and dispersed in alcohol, and a few drops of solution were added onto 200-mesh holey carbon copper grids. XPS measurements were performed using a VG Scientific ESCALab220i-XL instrument, using monochromatized Al K_α radiation at 300 W.

Supporting Information

Supporting Information is available from the Wiley Online Library or from the author.

Acknowledgements

[1] A. K. Geim, K. S. Novoselov, *Nat. Mater.* **2007**, *6*, 183.
[2] A. H. Castro Neto, N. M. R. Peres, K. S. Novoselov, A. K. Geim, *Rev. Mod. Phys.* **2009**, *81*, 109.
[3] C. Lee, X. Wei, J. W. Kysar, J. Hone, *Science* **2008**, *321*, 385.
[4] K. S. Kim, Y. Zhao, H. Jang, S. Y. Lee, J. M. Kim, K. S. Kim, J.-H. Ahn, P. Kim, J.-Y. Choi, B. H. Hong, *Nature* **2009**, *457*, 706.
[5] Y. M. Lin, C. Dimitrakopoulos, K. A. Jenkins, D. B. Farmer, H. Y. Chiu, A. Grill, P. Avouris, *Science* **2010**, *327*, 662.
[6] F. Schedin, A. K. Geim, S. V. Morozov, E. W. Hill, P. Blake, M. I. Katsnelson, K. S. Novoselov, *Nat. Mater.* **2007**, *6*, 652.
[7] Y.-M. Lin, K. A. Jenkins, A. Valdes-Garcia, J. P. Small, D. B. Farmer, P. Avouris, *Nano Lett.* **2008**, *9*, 422.
[8] M. Liu, X. Yin, E. Ulin-Avila, B. Geng, T. Zentgraf, L. Ju, F. Wang, X. Zhang, *Nature* **2011**, *474*, 64.
[9] S. K. Min, W. Y. Kim, Y. Cho, K. S. Kim, *Nat. Nanotechnol.* **2011**, *6*, 162.
[10] L. Liao, Y.-C. Lin, M. Bao, R. Cheng, J. Bai, Y. Liu, Y. Qu, K. L. Wang, Y. Huang, X. Duan, *Nature* **2010**, *467*, 305.
[11] Y. M. Lin, A. Valdes-Garcia, S. J. Han, D. B. Farmer, I. Meric, Y. Sun, Y. Wu, C. Dimitrakopoulos, A. Grill, P. Avouris, K. A. Jenkins, *Science* **2011**, *332*, 1294.
[12] R. R. Nair, H. A. Wu, P. N. Jayaram, I. V. Grigorieva, A. K. Geim, *Science* **2012**, *335*, 442.
[13] J. R. Miller, R. A. Outlaw, B. C. Holloway, *Science* **2010**, *329*, 1637.
[14] N. G. Shang, P. Papakonstantinou, M. McMullan, M. Chu, A. Stamboulis, A. Potenza, S. S. Dhesi, H. Marchetto, *Adv. Funct. Mater.* **2008**, *18*, 3506.
[15] J. J. Wang, M. Y. Zhu, R. A. Outlaw, X. Zhao, D. M. Manos, B. C. Holloway, V. P. Mammana, *Appl. Phys. Lett.* **2004**, *85*, 1265.
[16] N. Soin, S. Sinha Roy, S. Roy, K. S. Hazra, D. S. Misra, T. H. Lim, C. J. Hetherington, J. A. McLaughlin, *J. Phys. Chem. C* **2011**, *115*, 5366.
[17] W. Takeuchi, H. Kondo, T. Obayashi, M. Hiramatsu, M. Hori, *Appl. Phys. Lett.* **2011**, *98*, 123107.
[18] C.-K. Huang, Y. Ou, Y. Bie, Q. Zhao, D. Yu, *Appl. Phys. Lett.* **2011**, *98*, 263104.
[19] L. M. Malard, M. A. Pimenta, G. Dresselhaus, M. S. Dresselhaus, *Phys. Rep.* **2009**, *473*, 51.
[20] J. A. Leiro, M. H. Heinonen, T. Laiho, I. G. Batirev, *J. Electron Spectrosc* **2003**, *128*, 205.
[21] E.-S. Henriette, *Carbon* **2004**, *42*, 1713.
[22] J. A. Venables, G. D. T. Spiller, M. Hanbucken, *Rep. Prog. Phys.* **1984**, *47*, 399.
[23] G. Rosenfeld, R. Servaty, C. Teichert, B. Poelsema, G. Comsa, *Phys. Rev. Lett.* **1993**, *71*, 895.
[24] Z. Zhang, *Science* **1997**, *276*, 377.
[25] N. Ferralis, R. Maboudian, C. Carraro, *Phys. Rev. Lett.* **2008**, *101*, 156801.
[26] Z.-S. Wu, S. Pei, W. Ren, D. Tang, L. Gao, B. Liu, F. Li, C. Liu, H.-M. Cheng, *Adv. Mater.* **2009**, *21*, 1756.
[27] F. Liu, J. Tian, L. Bao, T. Yang, C. Shen, X. Lai, Z. Xiao, W. Xie, S. Deng, J. Chen, J. She, N. Xu, H. Gao, *Adv. Mater.* **2008**, *20*, 2609.
[28] S. Fan, M. G. Chapline, N. R. Franklin, T. W. Tombler, A. M. Cassell, H. Dai, *Science* **1999**, *283*, 512.
[29] P. Hojati-Talemi, G. P. Simon, *Carbon* **2011**, *49*, 2875.
[30] E. Stratakis, G. Eda, H. Yamaguchi, E. Kymakis, C. Fotakis, M. Chhowalla, *Nanoscale* **2012**, *4*, 3069.